Dramatic Increase of ^{3}MLCT State Lifetime of a Ruthenium(II) Polypyridine Complex upon Entrapment within Y-Zeolite Supercages

Krzysztof Maruszewski and James R. Kincaid*

Chemistry Department, Marquette University, Milwaukee, Wisconsin 53233

Received July 12, 1994[⊗]

A bis-heteroleptic, tris-ligated polypyridine complex of ruthenium(II) ($Ru(bpy)_2(daf)^{2+}$) has been prepared in zeolite Y supercages and investigated by electronic absorption, electronic emission, and resonance Raman spectroscopy. While liquid solutions of this complex exhibit very weak luminescence with excited-state lifetime shorter than 10 ns at room temperature, entrapment in zeolite supercage results in dramatic increases in emission intensity and lifetime (302 ns at room temperature), providing access to practically important potential photoredox reactivity of the complex. The observed temperature dependence of the excited-state lifetime has been modeled by a kinetic equation with two thermal terms corresponding to the so-called fourth ^{3}MLCT state and ligand field state (LF), respectively. It is shown that the increased lifetime of the entrapped complex results from zeolite-induced destabilization of the LF state, a conclusion which is in agreement with results obtained for a number of other zeolite-entrapped Ru(II) polypyridine complexes.

Introduction

The increasing interest in organized molecular assemblies,[1] along with the inherent potential of tris(polypyridine) complexes of ruthenium(II) for solar energy conversion schemes,[2] has prompted us[3] and others[4−6] to investigate the photophysical and photoredox properties of these complexes entrapped within the supercages of Y-zeolite. Such studies assume ever-increasing importance in light of the recent progress made by Dutta[4] and Mallouk[5] and their co-workers in achieving significant increases in photoredox efficiencies for such systems.

In an effort to expand the available range of structural variants for this class of materials, we had earlier developed a versatile synthetic scheme to produce a potentially wide range of bis-heteroleptic, tris-ligated sensitizers.[3a] In a subsequent work,[3b] the spectral and photophysical properties of a number of such species were documented and it was shown that the principal effect of the zeolite supercage is to destabilize the so-called ligand field (LF) state, thermal population of which leads to rapid and efficient nonradiative decay or (in solution) to deligation (*i.e.*, loss of sensitizer).[10−12]

As has been discussed in detail elsewhere,[3b] this LF state destabilization arises as a consequence of steric restrictions imposed by the fixed size of the supercage, an interpretation which was originally proposed by Meyer and co-workers to explain similar behavior of tris(bipyridine)ruthenium(II) in a rigid cellulose acetate matrix.[7] Thus, referring to Figure 1, the LF state, being anti-bonding in respect to the Ru−N bond, is expected to possess longer Ru−N bonds. In a rigid matrix (or within the spatially restricted zeolite supercage), the LF state is thus destabilized owing to the restriction to elongation. The energy dissipation via the LF channel is so efficient that, when present, it effectively masks the decay of the excited-state via the thermally induced fourth ^{3}MLCT state. An increase in the energy gap between the low-lying ^{3}MLCT states and the LF state renders the latter thermally inaccessible, allowing the fourth ^{3}MLCT state to dominate the temperature-dependent decay process. The actual values of the rate constants and energy gap shown in Figure 1 can be experimentally determined by conducting lifetime measurements over a wide range of temperatures, as is explained elsewhere.[3b]

The specific complexes studied in the earlier work[3b] all possessed inherently large (>3000 cm^{-1}) energy gaps between the low-lying ^{3}MLCT states and the LF state. Further destabilization by the zeolite supercage is apparently sufficient to effectively eliminate this decay pathway from the overall relaxation scheme, thereby preventing a determination of the energy gap for the entrapped complexes. In order to address this issue it is necessary to employ a complex whose inherent energy gap is sufficiently small that the further destabilization by the supercage will not prevent thermal population of the LF state. In this way it becomes possible (through analysis of the temperature-dependent lifetime data) to obtain a quantitative estimate of the degree of destabilization induced by the zeolite cavity.

Herein we report the results of such a study, employing the heteroleptic complex of ruthenium(II) with 2,2′-bipyridine (bpy) and diazafluorene (daf), *i.e.*, $Ru(bpy)_2(daf)^{2+}$. This complex is known to possess an inherently small (^{3}MLCT−LF) energy gap,

[⊗] Abstract published in *Advance ACS Abstracts,* March 15, 1995.

(1) (a) *Supramolecular Photochemistry*; Balzani, V., Ed.; NATO ASI Series C; D. Reidel Publishing Co.: Dordrecht, Holland, 1987. (b) Balzani, V.; Scandola, F. *Supramolecular Photochemistry*; Ellis Horwood Limited: Chichester, England, 1991. (c) *Photochemistry in Organized and Constrained Media*; Ramamurthy, V., Ed.; VCH Publishers, Inc.: New York, 1991.

(2) (a) Juris, A.; Balzani, V.; Barigelletti, F.; Champagna, S.; Belser, P.; von Zalewsky, *Coord. Chem. Rev.* **1988**, *84*, 85. (b) Kalyanasundaram, K. *Photochemistry of Polypyridine and Porphyrin Complexes*; Academic Press Limited: London, England, 1992.

(3) (a) Maruszewski, K.; Strommen, D. P.; Handrich, K.; Kincaid, J. R. *Inorg. Chem.* **1991**, *30*, 4579. (b) Maruszewski, K.; Strommen, D. P.; Kincaid, J. R. *J. Am. Chem. Soc.* **1993**, *115*, 8345.

(4) (a) DeWilde, W.; Peeters, G.; Lunsford, J. H. *J. Phys. Chem.* **1980**, *84*, 2306. (b) Quayle, W. H.; Lunsford J. H. *Inorg. Chem.* **1982**, *21*, 97.

(5) (a) Dutta, P. K.; Incavo, J. A. *J. Phys. Chem.* **1987**, *91*, 4443. (b) Incavo, J. A.; Dutta, P. K. *J. Phys. Chem.* **1990**, *94*, 3075. (c) Turbeville, W.; Robins, D. S.; Dutta, P. K. *J. Phys. Chem.* **1992**, *96*, 5024. (d) Dutta, P. K.; Turbeville, W. *J. Phys. Chem.* **1992**, *96*, 9410. (e) Borja, M.; Dutta, P. K. *Nature* **1993**, *362*, 43.

(6) (a) Li, Z.; Wang, C. H.; Persaud, L.; Mallouk, T. E. *J. Phys. Chem.* **1988**, *92*, 2592. (b) Kruger, J. S.; Mayer, J. A.; Mallouk, T. E. *J. Am. Chem. Soc.* **1988**, *110*, 8232. (c) Kim, Y.; Mallouk, T. E. *J. Phys. Chem.* **1992**, *96*, 2879.

(7) Lumpkin R. S.; Kober, E. M.; Worl, L. A.; Murtaza, Z.; Meyer, T. J. *J. Phys. Chem.* **1990**, *94*, 239.

0020-1669/95/1334-2002$09.00/0

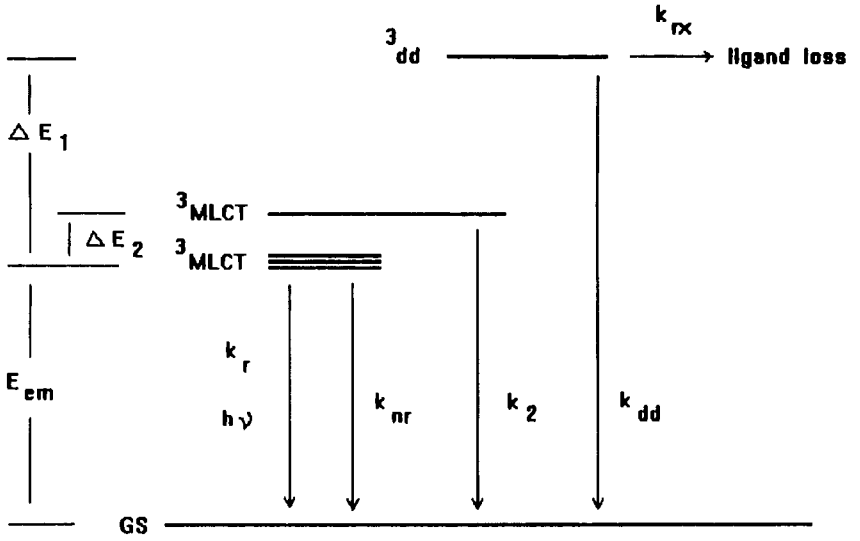

Figure 1. Schematic representation of the excited-state deactivation pathways in $Ru(bpy)_3^{2+}$.

owing to the weak donor strength of the daf ligand.[8] The results not only confirm the concepts and interpretation outlined above but, more importantly, nicely demonstrate the concept that zeolite entrapment provides a quite useful strategy for advantageous manipulation of the photophysical properties of such systems. Thus, in the present case, entrapment within the Y-zeolite supercage effectively "turns-on" emission originating from the ^{3}MLCT state and provides access to potentially important photophysical and photoredox characteristics of such species.

In order to ensure that increase in the observed emission intensity of the zeolite-entrapped $Ru(bpy)_2(daf)^{2+}$ complex is induced by increase in the ^{3}MLCT−LF energy gap (*i.e.*, longer lifetime), a sample of $Ru(bpy)_2(daf)^{2+}$ adsorbed on the surface of zeolite Y was prepared. Emission and lifetime measurements performed on this sample showed no significant differences as compared to the free complex. Thus, the interaction with the zeolite surface does not suffice to drastically influence the electronic states of $Ru(bpy)_2(daf)^{2+}$ and induce a significant increase in the observed lifetime and emission intensity.

Experimental Section

A. Materials. The Y zeolite was generously provided by the Union Carbide Corp., Danbury, CT. $Ru(NH_3)_6Cl_3$ was purchased from the Johnson Matthey Gmbh, Karlsruhe, Germany. 2,2′-Bipyridine (bpy) was purchased from the Aldrich Chemical Co., Milwaukee, WI. The bpy ligand was sublimed prior to use. 4,5-Diazafluorene (daf) ligand was prepared by using literature methods.[9]

B. Preparation of Compounds. The syntheses of zeolite-entrapped polypyridine complexes have been described previously,[3] and $Ru(bpy)_2(daf)^{2+}$−Y was prepared by an analogous procedure. One important modification of the procedures described earlier was the addition of a 72 h soxhlet extraction (with 95% EtOH) of $Ru(bpy)_2^{2+}$−Y in order to remove traces of bpy ligand. All physical measurements, with the exception of diffuse reflectance spectra, were conducted on samples prepared as described in ref 3b. Diffuse reflectance data were obtained from KBr pellets prepared as for standard IR measurements. The zeolite-entrapped complex was extracted from the zeolite matrix by the hydrofluoric acid method described in ref 3a. The integrity of the zeolite-entrapped sample was confirmed as described previously[3] by RR, electronic absorption, and emission spectra as well as by TLC. The free $Ru(bpy)_2(daf)^{2+}$ complex was prepared by literature methods.[9]

The $Ru(bpy)_2(daf)^{2+}$ complex adsorbed on the surface of zeolite Y was prepared by the method described by Kim and Mallouk.[6c] Briefly, 0.2 g of zeolite Y was suspended with stirring in 10 mL of a 6.0×10^{-5} molar aqueous solution of $Ru(bpy)_2(daf)^{2+}Cl_2$. The suspension was stirred for ~15 min and allowed to stand overnight. The sample was then filtered out, repeatedly washed with deionized water and air-dried. Comparison of the absorption spectra of the zeolite extracts showed that the total concentration of $Ru(bpy)_2(daf)^{2+}$ in the case of the adsorbed complex was ~15 times smaller than that of the incorporated $Ru(bpy)_2(daf)^{2+}$. Thus, the concentration of $Ru(bpy)_2(daf)^{2+}$ adsorbed on the surface of zeolite Y was ≤ 0.53 μM/1 g of zeolite. This ensures that much less than a monolayer of the complex was formed on the surface of zeolite since monolayer coverage for $Ru(bpy)_3^{2+}$ on zeolite Y was known to be approximately 7.0 μM/1 g of zeolite.[6c]

C. Spectroscopic Measurements. Resonance Raman spectra and electronic absorption and emission data were obtained as previously described.[3b] Diffuse reflectance UV−vis spectra were taken in transmission mode with a Perkin-Elmer 320 spectrophotometer equipped with a Hitachi integrating sphere attachment. Samples were referenced to plain Y zeolite. Spectra were Kubelka−Munk corrected using Spectra Calc software.

Excited-state lifetimes were obtained using a Spex Model 340S spectrograph equipped with an RCA C31034A-02 photomultiplier tube. The 354.7-nm radiation from a Quanta-Ray (Spectra-Physics) Model DCR-3 Nd:YAG laser (operated at 20 Hz) with the beam defocused was used as the excitation source. The photomultiplier tube output signal was directed to a LeCroy 9450A digital oscilloscope. Usually 500 sweeps were collected and averaged, yielding a time-dependent decay curve. The data were then transferred to a PC computer and fitted (within approximately 4τ) to biexponential curves (vide infra) by a PSI-Plot program.

The excited-state lifetimes were acquired at various temperatures with the aid of a cold cell of in-house design, which consists of a dewar containing an NMR tube spinner. The dewar was filled with ethanol/dry ice cooling slurry, and an NMR tube containing the zeolite sample was then immersed. The sample temperature was allowed to equilibrate for at least 15 min, and as the temperature of the cooling slurry was allowed to rise slowly, the decay curves were measured at various temperatures. Analogously, for lifetime measurements at temperatures higher than 25 °C, hot water was used as the thermal bath. The temperature inside the dewar was monitored by a TEGAM 821 microprocessor thermometer equipped with a J thermocouple. The rate of temperature rise typically did not exceed 0.4 °C/min in the −70 to 25 °C range, and temperature variations during signal acquisition (~20 s) did not exceed 0.5 °C. It was established that with the experimental conditions described above the temperature difference between the zeolite sample and the surrounding medium did not exceed 0.5 °C.

(8) (a) Henderson, L. J., Jr.; Fronczek, F. R.; Cherry, W. R. *J. Am. Chem. Soc.* **1984**, *106*, 5876. (b) Wacholtz, W. M.; Auerbach, R. A.; Schmehl, R. H.; Ollino, M.; Cherry, W. R. *Inorg. Chem.* **1985**, *24*, 1758.

(9) Danzer, G. D. Ph.D. Dissertation, Marquette University, Milwaukee, WI, 1990.

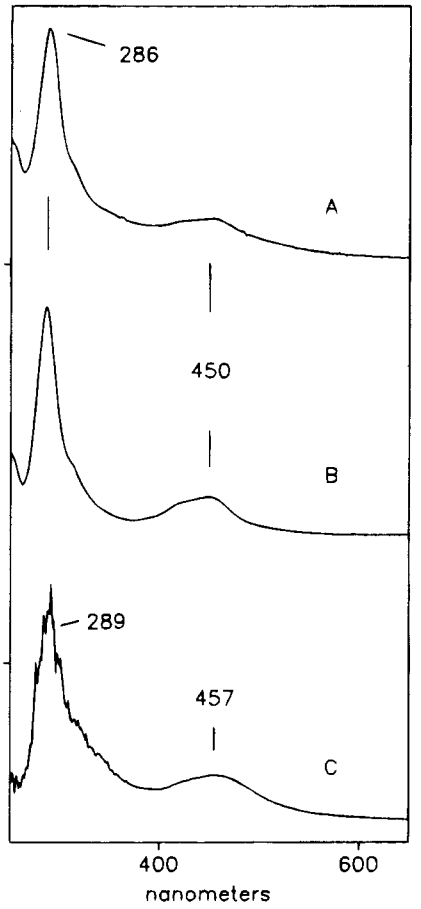

Figure 2. Electronic absorption spectra of aqueous solutions of Ru(bpy)$_2$(daf)$^{2+}$ extracted from zeolite (trace A) and independently synthesized complex (trace B). Trace C presents diffuse reflectance spectrum of the zeolite-entrapped complex.

The temperature-dependent lifetime data were fitted to multiexponential kinetic expressions by a PSI-Plot program.

Results

A. Electronic Spectra. The electronic absorption and emission spectra of the complex in various forms are given in Figures 2 and 3. The absorption spectrum of the synthesized complex in aqueous solutions, given in trace B of Figure 2, matches that reported in the literature.[8] The diffuse reflectance spectrum (trace C) of the zeolite-entrapped complex exhibits a slight red shift in the MLCT transition (450 vs 457 nm), behavior which is consistent with that seen previously for other zeolite-entrapped homo- and heteroleptic complexes.[3b] In trace A is given the electronic absorption spectrum of the liberated complex, following dissolution of the zeolite matrix, and it is clear that this spectrum matches that in trace B, demonstrating the fact that the red shift is indeed attributable to the effects of the zeolite matrix.

The emission spectra given in Figure 3 illustrate the fact that there is a substantial increase in luminescence upon entrapment in zeolite. The emission intensity from the solution samples is extremely weak, a result that is in agreement with previous work.[8] Comparing traces A and B gives evidence of a slight red shift (620 vs 610 nm) for the zeolite-entrapped species, a result which is also consistent with the results reported previously for other zeolite-entrapped species.[3b]

B. Resonance Raman (RR) Spectra. The RR spectra of the complex in solution and that of the zeolite-entrapped species are given in Figure 4. Comparison of these spectra shows there are slight shifts ($\leq$4 cm^{-1}) observed for the zeolite-entrapped

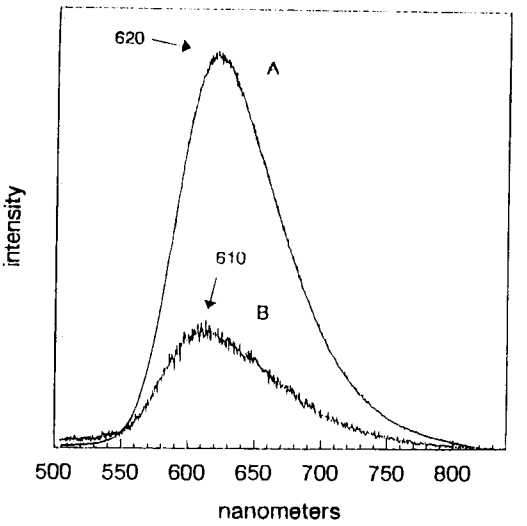

Figure 3. Electronic emission spectra of Ru(bpy)$_2$(daf)$^{2+}$−Y (trace A) and an aqueous solution of independently synthesized complex (trace B). The spectrum presented in trace B was multiplied by factor of 18. The spectrum of Ru(bpy)$_2$(daf)$^{2+}$ extracted from zeolite is superimposable with trace B.

complex relative to the features observed in solution, and the exact agreement between the two solution spectra confirms the identity of the entrapped complex.

C. Lifetime Data. The ^{3}MLCT state lifetime of Ru(bpy)$_2$(daf)$^{2+}$ in liquid solutions[8] is too short to be recorded on the nanosecond time scale (<10 ns) at room temperature. However, the strong luminescence of the zeolite-entrapped sample at room temperature has an associated lifetime of 302 ns in aqueous suspension. It is noted that the surface-adsorbed sample exhibits no significant differences in emission maxima and lifetimes from the complex in liquid solution. Thus, the effect of the zeolite is attributed to entrapment within the supercage rather than to interaction with the zeolite surface. As in the case of some other zeolite-entrapped complexes,[3b,5c] it was necessary to apply a biexponential model of the decay to reproduce the observed decay curves, with a short living component (~100 ns) contributing approximately 30% of the initial emission intensities. Excited-state lifetimes obtained at low temperatures increase, as expected, with decreasing temperature, reaching 1804 ns at −65 °C. Figure 5 presents semilogarithmic plots of the decay curves obtained at room temperature and −65 °C.

Discussion

A. Integrity of the Entrapped Complex. All of the spectral results are consistent with the proposed identity of the entrapped complex. Thus, both the absorption and emission spectra (Figure 2 and 3) yield λ_{max} values close to those observed by us and others[8] for the Ru(bpy)$_2$daf^{2+} complex. The slight shifts observed for the zeolite-entrapped species, relative to the solution values, are very similar to those observed for other entrapped complexes and presumably result from small alterations in ligand π^* orbital energies.[3b]

The virtual identity of the frequencies observed in the ground-state RR spectrum (Figure 4) of the complex in solution with those of the zeolite-entrapped species indicates insignificant differences in the ground-state structure of the complex in the two environments. The small, but significant, differences in the relative intensities between the two spectra reflect the excited-state changes implicated in the electronic spectral results discussed above. This behavior also has been previously noted for other zeolite-entrapped complexes.[3,5]

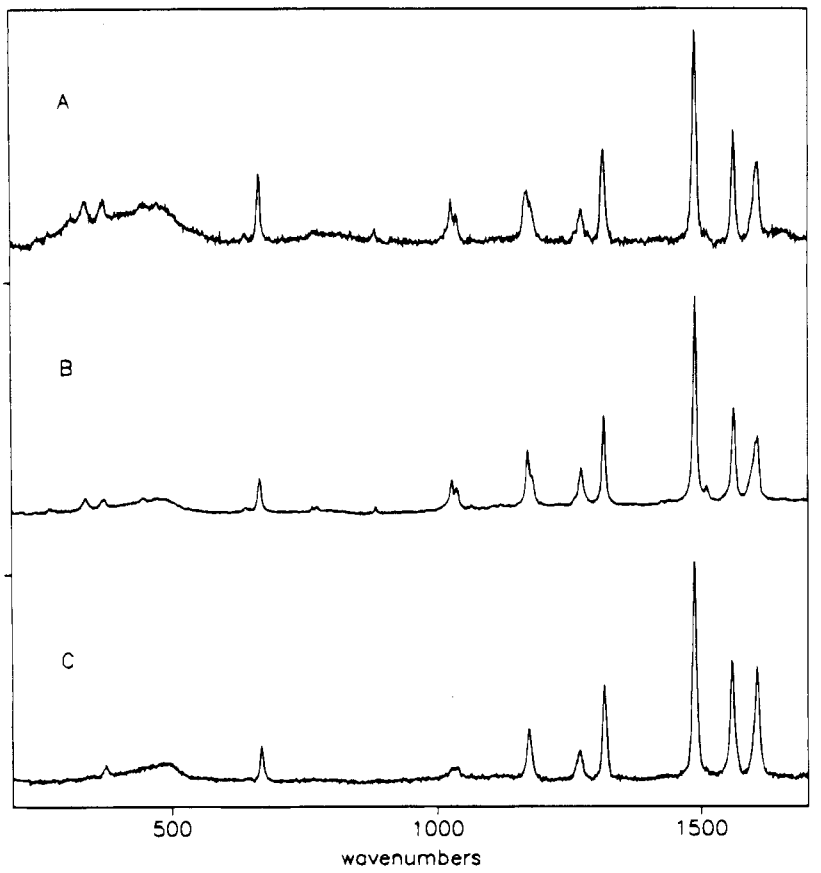

Figure 4. Resonance Raman spectra (with 457.9-nm excitation) of $Ru(bpy)_2(daf)^{2+}$ extracted from zeolite (trace A), independently prepared (trace B) and entrapped in zeolite (trace C).

In summary, as judged by electronic absorption, emission, and RR spectra, the zeolite-entrapped complex experiences only minor, if any, structural changes upon entrapment. Obviously, the key information needed to reveal the factors which lead to the observed lifetime increase is accessible only through the measurement of the temperature dependence of the lifetime, as is discussed below.

B. Photophysics. As is depicted in Figure 1, the ^{3}MLCT excited-state has alternate thermally-dependent decay pathways available to it in addition to the radiative (k_r) and direct nonradiative (k_{nr}) terms.

$$1/\tau = k_{tot.} = k_r + k_{nr} + k_1\Delta E_1 + k_2\Delta E_2 \qquad (1)$$

Table 1 lists kinetic data obtained for $Ru(bpy)_3^{2+}$ in different environments. Entrapment of the complex in zeolite[3b] or embedding it in a rigid cellulose acetate[7] matrix rendered the LF state inaccessible, while in liquid solutions (propylene carbonate[10] and EtOH[11]) the LF state dominates the decay. The relevant energy gap (ΔE_2) is determined by the donor strengths and LUMO energies of the constituent chelate ligands. For example, the ΔE_2 for propylene carbonate solutions of $Ru(bpm)_3^{2+}$ (where bpm = 2,2′-bipyrimidine) has been determined[100] to be 3375 cm^{-1}, whereas for $Ru(bpm)_2(bpy)^{2+}$ it is 3800 cm^{-1}. That is, in both cases the ^{3}MLCT state is localized on a bpm ligand, but the ΔE_2 is larger for the latter complex, because the energy of the LF state is raised as a consequence of the increased donor strength of bpy, relative to bpm.

In the specific case of interest here, $Ru(bpy)_2(daf)^{2+}$, the daf ligand is known to possess a relatively weak ligand field as a consequence of steric restrictions to N−Ru−N bond alignment, which arise because of the rigid methylene bridge between the 3-positions of the pyridine rings.[8] The most important consequence of this is that complexes which are constituted with this ligand will generally possess a smaller energy gap (ΔE_2) than a similar complex in which the daf ligand is replaced by one with a higher field strength. For the specific case in point, the ΔE_2 obtained[8b] for $Ru(bpy)_2(daf)^{2+}$ in EtOH/MeOH is equal to 2271 cm^{-1}, while $Ru(bpy)_3^{2+}$ in the same medium possesses[8b] a ΔE_2 of 3859 cm^{-1}.

In the model used for fitting of the observed lifetimes, the temperature-independent terms (k_r and k_{nr}) in eq 1 were replaced by a single linear term k. Two expressions were tested in an attempt to reproduce the observed data. One of them contained the linear term k and a single exponential term while the other possessed the linear term and both temperature-dependent terms (eq 1). Figure 6 presents the results of the fitting. Analysis of the curves shown in Figure 6 reveals that the monoexponential model (single thermal term) does not satisfactorily reproduce the observed lifetime data. However, introduction of the second thermal term yields excellent agreement between the calculated and observed curves.

The kinetic parameters obtained from both models are given in Table 1. Comparison of the ΔE_2 values for solution phase[8] $Ru(bpy)_2(daf)^{2+}$ and the zeolite-entrapped complex shows a substantial increase upon zeolite entrapment (1737 cm^{-1}). This observation accounts for the dramatic increase in lifetime and emission intensity upon zeolite entrapment. The steric constraint induced by the rigid zeolite cage on the electronically excited $Ru(bpy)_2(daf)^{2+}$−Y results in destabilization of the LF state,[3b] leading to a decrease in thermal population of this state.

(10) (a) Caspar, J. V.; Meyer, T. J. *J. Am. Chem. Soc.* **1983**, *105*, 5583. (b) Allen, G. H.; White, R. P.; Rillema, D. P.; Meyer, T. J. *J. Am. Chem. Soc.* **1984**, *106*, 2613.
(11) Van Houten, J.; Watts, R. J. *J. Am. Chem. Soc.* **1976**, *98*, 4853.
(12) Allsopp, S. R.; Cox, A; Kemp, T. J.; Reed, W. J. *J. Chem. Soc., Faraday Trans. 1* **1978**, *74*, 1275.

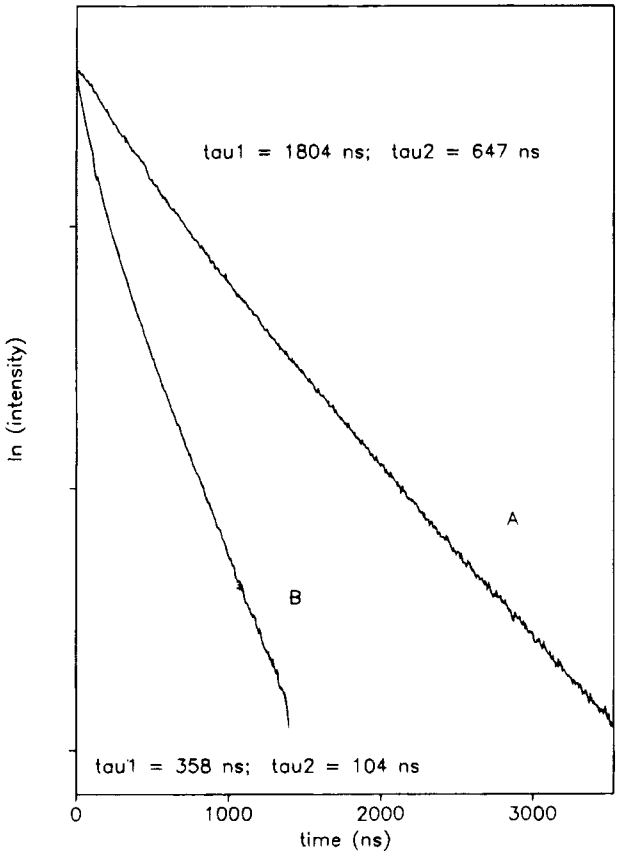

Figure 5. Logarithmic plots of the emission decay curves obtained for $Ru(bpy)_2(daf)^{2+}-Y$ at −65 °C (trace A) and at 17 °C (trace B). The decay curves posses biexponential character.

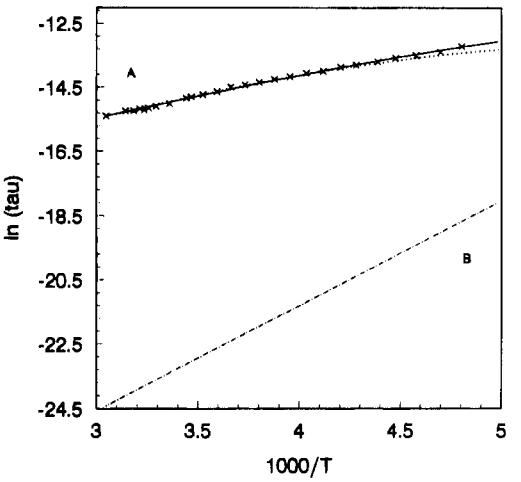

Figure 6. Temperature-dependent lifetime data obtained for $Ru(bpy)_2(daf)^{2+}$ in zeolite matrix (trace A) and in EtOH/MeOH solution (trace B).[8b] The experimental points are marked by "×". The solid line in trace A was generated from eq 1 using two thermal terms; the dotted line was obtained with one thermal term. The kinetic parameters are given in Table 1.

Table 1. Photophysical Parameters

compd	$k_r + k_{nr}$, $s^{-1} \times 10^5$	k_1, $s^{-1} \times 10^{12}$	ΔE_1, cm^{-1}	k_2, $s^{-1} \times 10^7$	ΔE_2, cm^{-1}
$Ru(bpy)_3^{2+}-Y^a$	3.8			11	890
$Ru(bpy)_3^{2+}-CA^b$	10			1.7	810
$Ru(bpy)_3^{2+}-PC^c$	6.1	4	3275		
$Ru(bpy)_3^{2+}-Et^d$	5.4	245	4046		
$Ru(bpy)_2(daf)^{2+}$ [e]	3.1	850	2271		
$Ru(bpy)_2(daf)^{2+}-Y^f$	1.8	0.8	4008	36.4	994
$Ru(bpy)_2(daf)^{2+}-Y^g$	4.2			63.2	1128

[a] Entrapped in zeolite; data from ref 3b. [b] In cellulose acetate; data from ref 7. [c] In propylene carbonate; data from ref 10b. [d] In EtOH; from ref 12. [e] In EtOH/MeOH; from ref 8b. [f] Entrapped in zeolite; fitted using two thermal terms. [g] Entrapped in zeolite; fitted using one thermal term.

It is instructive to consider the general consequences of this zeolite-induced ligand-field state destabilization, assuming a relatively constant effect for these types of complexes. For example, in a previous work,[3b] such data were reported for a more extensive set of complexes, wherein the inherent ΔE_2 value (*i.e.*, for the solution phase complexes) was ~3300 cm^{-1}. Assuming a relatively constant effect for zeolite-induced LF state destabilization of ~1700 cm^{-1}, all of the entrapped complexes reported there are expected to possess ΔE_2 values greater than 5000 cm^{-1}. Using the general destabilization factor derived from the present work (*i.e.*, 1737 cm^{-1}) and the resultant lowest expected ΔE_2 for that group (*i.e.*, ΔE_2 = 5012 cm^{-1}), eq 1 predicts the contribution from this pathway to be ~0.02% at room temperature; *i.e.*, it is effectively eliminated in those cases.

Conclusions and Implications

The present study not only provides an estimate of the magnitude of the zeolite-induced destabilization factor for such complexes but also clearly demonstrates that such entrapment can alter inherent photophysical properties of the complex in an advantageous manner. Thus, for the specific case in point, a complex which possesses quite unfavorable inherent photophysical properties (*i.e.*, short ^{3}MLCT state lifetime and the attendant high susceptibility to photo-induced ligand loss) is easily "converted" to a more promising photosensitizer by incorporation into the Y-zeolite supercage.

Acknowledgment. This work was supported by a grant from the Department of Energy, Office of Basic Energy Sciences (Grant ER13619). Such support does not constitute an endorsement by the DOE of the views expressed in this work.

IC9408213